Electronic Supplementary Information (ESI)

Materials and Instruments

All the chemicals and reagents were purchased from commercial sources and used as received without further purification. The final products were subjected to vacuum sublimation to further improve purity before photoluminescence (PL) and electroluminescence (EL) properties investigations. ^{1}H and ^{13}C NMR spectra were measured on a Bruker AV 500 spectrometer in CD_2Cl_2 at room temperature. High resolution mass spectra (HRMS) were recorded on a GCT premier CAB048 mass spectrometer operating in MALDITOF mode. UV-vis absorption spectrum was measured on a Shimadzu UV-2600 spectrophotometer. PL spectra were recorded on a Horiba Fluoromax-4 spectrofluorometer. PL quantum yields were measured using a Hamamatsu absolute PL quantum yield spectrometer C11347 Quantaurus_QY. Transient PL decay spectra were measured using Quantaurus-Tau fluorescence lifetime measurement system (C11367-03, Hamamatsu Photonics Co., Japan). Cyclic voltammogram was measured in a solution of tetra-*n*-butylammonium hexafluorophosphate (nBu$_4$NPF$_6$, 0.1 M) in acetonitrile containing the sample at a scan rate of 100 mV s^{-1}. Three-electrode system (Ag/Ag$^+$, platinum wire and glassy carbon electrode as reference, counter and work electrode respectively) was used in the CV method. HOMO = $-[E_{ox} + 4.8]$ eV, and LUMO = $-[E_{re} + 4.8]$ eV. E_{ox} and E_{re} represent the onset oxidation and reduction potentials relative to Fc/Fc$^+$, respectively. The ground-state geometries were optimized using the density function theory (DFT) method with PBEO functional at the basis set level of 6-31G*, and the ΔE_{ST} values were calculated by time-dependent DFT (TDDFT) method at the PBEO/6-31G* level. All the calculations were performed using Gaussian09 package.

Device Fabrication and Measurement

The glass substrates precoated with a 90-nm layer of indium tin oxide (ITO) with a sheet resistance of 15~20 Ω per square were successively cleaned in ultrasonic bath of acetone, isopropanol, detergent and deionized water, respectively, taking 10 minutes for each step. Then, the substrates were totally dried in a 70 °C oven. Before the fabrication processes, in order to improve the hole injection ability of ITO, the substrates were treated by O_2 plasma for 10 minutes. The vacuum-deposited OLEDs were fabricated under a pressure of $< 5 \times 10^{-4}$ Pa in the Fangsheng OMV-FS450 vacuum deposition system. Organic materials, LiF and Al were deposited at rates of 1~2 A s^{-1}, 0.1 A $s^{-1}$and 5 A s^{-1}, respectively. The effective emitting area of the devices was 9 mm^2, determined by the overlap between anode and cathode. The luminance–voltage–current density characteristics and EL spectra were obtained via a Konica Minolta CS-200 Color and Luminance Meter and an Ocean Optics USB 2000+ spectrometer, along with a Keithley 2400 Source Meter. The external quantum efficiencies were estimated utilizing the normalized EL spectra and the current efficiencies of the devices, assuming that the devices are Lambertian emitters. All the characterizations were conducted at room temperature in ambient conditions without any encapsulation, as soon as the devices were fabricated.

Additional Spectra and Tables

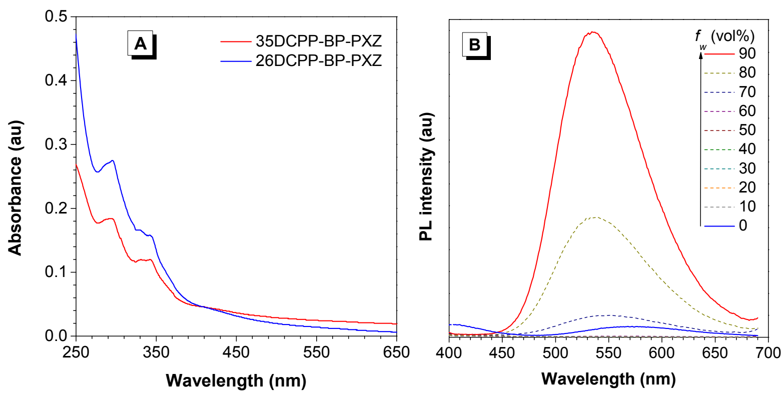

Fig. S1 (A) Absorption spectra of the new compounds in neat film; (B) PL spectra of 35DCPP-BP-PXZ in THF/water mixtures with different water fractions (f_w).

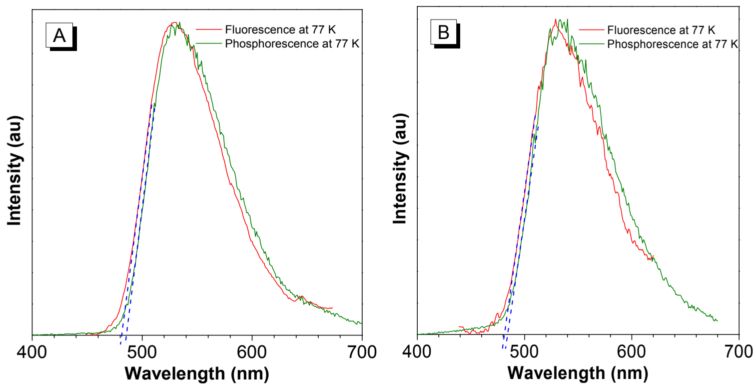

Fig. S2 Fluorescence and phosphorescence spectra of neat films of (A) 35DCPP-BP-PXZ and (B) 26DCPP-BP-PXZ, measured at 77 K under nitrogen.

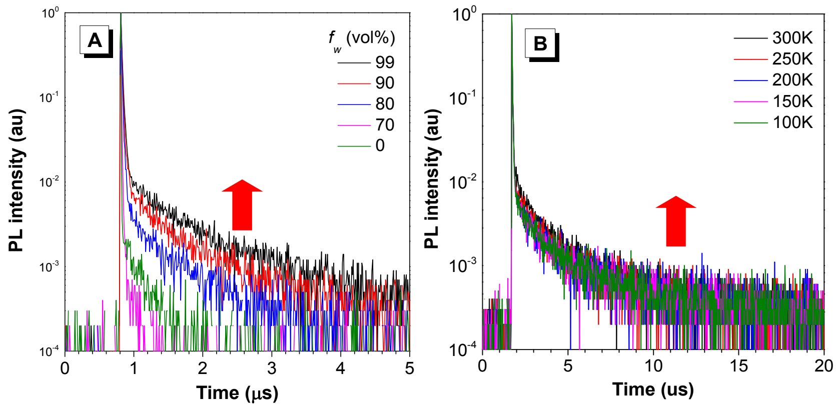

Fig. S3 (A) Transient PL decay curves of 26DCPP-BP-PXZ in THF/water mixtures with different water fractions (f_w) (10^{-5} M), measured under nitrogen. (B) Temperature-dependent transient PL decay spectra of 26DCPP-BP-PXZ in neat film, measured under nitrogen.

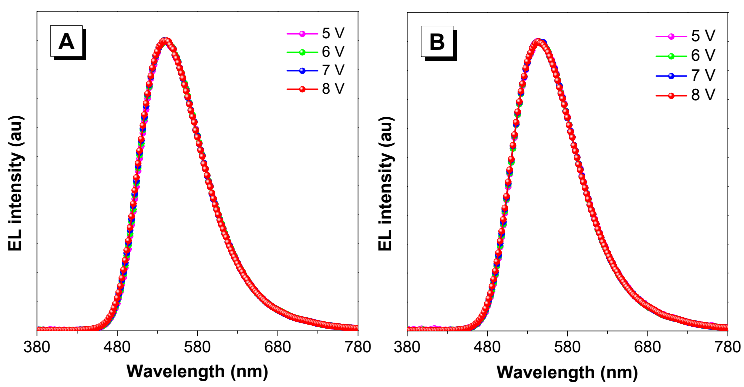

Fig. S4 EL spectra of nondoped OLEDs of (A) 35DCPP-BP-PXZ and (B) 26DCPP-BP-PXZ at varied voltages.

Estimation of Basic Photophysical Data

The quantum efficiencies and rate constants were determined using the following equations according to the following equations:

$$\Phi_{prompt} = \Phi_{PL}R_{prompt} \quad (1)$$

$$\Phi_{delayed} = \Phi_{PL}R_{delayed} \quad (2)$$

$$k_F = \Phi_{prompt}/\tau_{prompt} \quad (3)$$

$$\Phi_{PL} = k_F/(k_F + k_{IC}) \quad (4)$$

$$\Phi_{prompt} = k_F/(k_F + k_{IC} + k_{ISC}) \quad (5)$$

$$\Phi_{IC} = k_{IC}/(k_F + k_{IC} + k_{ISC}) \quad (6)$$

$$\Phi_{ISC} = k_{ISC}/(k_F + k_{IC} + k_{ISC}) = 1 - \Phi_{prompt} - \Phi_{IC} \quad (7)$$

$$\Phi_{RISC} = \Phi_{delayed}/\Phi_{ISC} \quad (8)$$

$$k_{RISC} = (k_p k_d \Phi_{delayed})/(k_{ISC}\Phi_{prompt}) \quad (9)$$

$$k_p = 1/\tau_{prompt};\ k_d = 1/\tau_{delayed} \quad (10)$$

Table S1. Transient PL decay data of 35DCPP-BP-PXZ and 26DCPP-BP-PXZ in THF/water mixtures solutions with different water fractions (f_w).[a]

compound	f_w	$\langle\tau\rangle$ (ns)	τ_1 (ns)	τ_2 (ns)	A_1	A_2	$\tau_{delayed}$ (ns)	$R_{delayed}$ (%)
35DCPP-BP-PXZ	0	1.8	1.8	–	153504.0	–	–	–
	70	10.4	8.3	55.7	17819.8	121.5	55.7	4.4
	80	82.6	15.9	521.8	14376.2	66.4	521.8	13.2
	90	151.1	18.7	705.3	13932.4	88.3	705.3	19.3
	99	174.9	19.0	745.8	13513.5	94.0	745.8	21.4
26DCPP-BP-PXZ	0	2.4	2.4	–	564256	–	–	–
	70	4.8	4.8	–	93097.9	–	–	–
	80	61.6	13.3	547.4	19850.1	48.0	547.4	9.0
	90	113.5	16.4	625.2	17263.2	85.8	625.2	15.9
	99	202.3	19.4	835.8	15496.2	103.8	835.8	22.4

[a] Transient PL decay data are fitted by multiple-exponential function and the mean fluorescence lifetimes ($\langle\tau\rangle$) were calculated by $\langle\tau\rangle = \Sigma A_i\tau_i^2/\Sigma A_i\tau_i$, where A_i is the pre-exponential for lifetime τ_i. $R_{delayed}$ is the delayed component ratio of fluorescence. $R_{delayed} = \tau_1 A_1/(\tau_1 A_1 + \tau_2 A_2)$.

Table S2. Transient PL decay data of 35DCPP-BP-PXZ and 26DCPP-BP-PXZ in neat film at different temperatures. [a]

compound	T (K)	$<\tau>$ (ns)	τ_1 (ns)	τ_2 (ns)	A_1	A_2	$\tau_{delayed}$ (ns)	$R_{delayed}$ (%)
35DCPP-BP-PXZ	100	174.9	24.7	1441.6	21509.8	43.7	1441.6	10.6
	150	204.0	25.4	1399.7	21232.8	57.5	1399.7	13.0
	200	363.6	24.8	1892.2	21548.4	62.5	1892.2	18.1
	250	403.1	24.0	1688.9	21850.8	91.4	1688.9	22.8
	300	412.8	22.3	1575.6	23005.5	111.3	1575.6	25.5
26DCPP-BP-PXZ	100	259.2	25.4	1647.4	21492.8	55.8	1647.4	16.2
	150	246.8	25.5	1527.1	21133.6	61.0	1527.1	14.4
	200	252.0	24.9	1541.2	21532.5	61.3	1541.2	14.7
	250	316.6	25.3	1640.4	21450.1	72.8	1640.4	18.0
	300	388.9	25.1	1684.3	21772.3	91.0	1684.3	21.9

[a] Transient PL decay data are fitted by multiple-exponential function and the mean fluorescence lifetimes ($<\tau>$) were calculated by $<\tau> = \Sigma A_i\tau_i^2/\Sigma A_i\tau_i$, where A_i is the pre-exponential for lifetime τ_i. $R_{delayed}$ is the delayed component ratio of fluorescence. $R_{delayed} = \tau_1 A_1/(\tau_1 A_1 + \tau_2 A_2)$.

Table S3. Photophysical data of 35DCPP-BP-PXZ and 26DCPP-BP-PXZ in THF and neat films.[a]

	35DCPP-BP-PXZ		26DCPP-BP-PXZ	
	THF	film	THF	film
Φ_{PL} (%)	2.2	66.5	2.7	67.9
τ_{prompt} (ns)	1.8	22.3	2.4	25.1
$\tau_{delayed}$ (μs)	–	1.58	–	1.68
$R_{delayed}$ (%)	–	25.5	–	21.9
Φ_{prompt} (%)	2.2	49.5	2.7	53.0
$\Phi_{delayed}$ (%)	–	17.0	–	14.9
Φ_{ISC} (%)	–	25.5	–	21.9
Φ_{RISC} (%)	–	66.5	–	67.9
k_F ($\times10^6$ s^{-1})	12.6	22.2	6.7	21.1
k_{IC} ($\times10^6$ s^{-1})	562	11.2	241	10.0
k_{ISC} ($\times10^6$ s^{-1})	–	11.4	–	8.8
k_{RISC} ($\times10^5$ s^{-1})	–	8.5	–	7.6

[a] Abbreviations: Φ_{PL} = absolute photoluminescence quantum yield; τ_{prompt} and $\tau_{delayed}$ = lifetimes calculated from the prompt and delayed fluorescence decay, respectively; $R_{delayed}$ = the ratio of delayed components; Φ_{prompt} and $\Phi_{delayed}$ = prompt and delayed components, respectively, determined from the total Φ_{PL} and the proportion of the integrated area of each component in the transient spectra to the total integrated area; Φ_{ISC} = the intersystem crossing quantum yield; k_F = fluorescence decay rate; k_{IC} = internal conversion decay rate from S_1 to S_0; k_{ISC} = intersystem crossing decay rate from S_1 to T_1; k_{RISC} = the rate constant of reverse intersystem crossing process.